RESEARCH ARTICLE

Application of response surface methodology for optimization of fluoride adsorption from aqueous solution using MgO-based nanocomposites

Somayeh Rahdar[1], Leili Mohammadi[2], Abbas Rahdar[3*], Shahin Ahmadi[4], Saeideh Sistani[4], Md. Abu Bin Hasan Susan[5]

[1] Department of Environmental Health, Zabol University of Medical Sciences, Zabol, Iran

[2] Assistant professor of Environmental Health, Infectious Diseases and Tropical Medicine Research Center, Resistant 8 Tuberculosis Institute, Zahedan University of Medical Sciences, Zahedan, Iran.

[3] Department of Physics, University of Zabol, Zabol, Iran

[4] MSc of Environmental Health, Kerman University of Medical Sciences, Kerman, Iran

[5] Department of Chemistry, University of Dhaka, Dhaka 1000, Bangladesh

ARTICLE INFO

Article History:
Received 2019-07-20
Accepted 2020-01-14
Published 2020-05-01

Keywords:
Fluoride
MgO-FCN-NPs
Response Surface
Methodology
Isotherm
Kinetic

ABSTRACT

Deleterious effect of high concentration fluoride in water resources on the health of human. The MgO supported Fe-Co-Mn nanoparticles were produced via co-precipitation method and characterized by SEM and FTIR techniques. In the work, the adsorption process optimization was performed by response surface modeling with the help of Minitab 16 software. The effect of independent parameters such as pH (3-11), the initial dose (0.02-0.1 g/L), the initial concentration of the fluoride (10-50 mg/L) and reaction time (30-180 min) were optimized to obtain the best response of fluoride removal using the statistical Box-Behnken in response surface modeling procedure. Conditions for the pH(5), the initial concentration of nanoparticle (0.05 g/L), the initial concentration of fluoride (50 mg/L) and the process time(90 min) were obtained as Min respectively. Under these conditions, the removal efficiency of the fluoride by MgO capped Fe-Co-Mn nanoparticles equal to 84.64% were achieved. ANONA high correlation coefficients for the proposed model was also obtained (adjusted –R2=0.9993 and R2=0.9984). The equilibrium data were analyzed using Langmuir, Freundlich, Temkin and Dubinin-Radushkevich isotherm models. The Langmuir model was found to be describing the data. Kinetic studies showed that the adsorption followed a pseudo-second order reaction.

How to cite this article
Rahdar S., Mohammadi L., Rahdar A., Ahmadi Sh., Sistani S., Hasan Susan A.B. Application of response surface methodology for optimization of fluoride adsorption from aqueous solution using MgO-based nanocomposites. J. Nanoanalysis., 2020; 7(2): 105-116. DOI: 10.22034/JNA.2020.1874451.1149.

INTRODUCTION

Fluoride is introduced into groundwater and surface water resources through wastewaters of iron, glass making, steel making, fertilizer, and aluminum making industries (1,2). Presence of fluorine at low concentrations in water resources has considerable effects in supplying and preserving the health of bones and teeth (3,4). WHO has limited the standard level of fluorine in drinking water to 1.5 mg/L, with lower values stated for children (5,6). Fluoride in the human body, given the duration of exposure, leads to dental fluorosis and skeletal fluorosis. Dental fluorosis which, is more specific to children leads to increased enamel porosity, diminished mineral content of teeth, and vulnerability of teeth (7-9). Further, fluoride causes other diseases such as osteoporosis, infertility, etc. (10, 8-12). It also affects the metabolism of other elements such as calcium and potassium in the body (13). High fluoride concentrations in

* Corresponding Author Email: *a.rahdar@uoz.ac.ir*
a.rahdarnanophysics@gmail.com

ground waters in 30 countries have caused more than 260 million people to experience health problems (14). Thus, use of different technologies for defluorination from water resources with high fluorine concentration or those contaminated with fluoride is essential (3). Various methods have been developed for fluoride removal categorized as absorption, membrane processes, coagulation and chemical precipitation, nanofiltration, reverse osmosis, and ion exchange (15-18). The selection of each of these methods depends on the concentration, region, and water resources available (12). Coagulation and precipitation are cheaper, but they cause production of harmful materials. On the other hand, membrane processes such as reverse osmosis have a high maintenance cost, and the ion exchange is very costly (19). Among these methods adsorption is a widely used method for defluoridation which depend on ions (adsorbate) in liquid diffusing to the surface of a solid (adsorbent)(9).

Adsorption is known as the most fundamental and efficient method which is environmentally friendly, inexpensive, efficient, and easy in operation (17, 20, 21). Adsorption technique for fluoride removal by using several adsorbents such as activated carbon, bentonite, red mud, iron oxide, zeolites, fly ash and charcoals (22-24). In the current study, the nanoparticles of MgO-FCN were synthesized via co-precipitation method. Their structural and magnetic properties were studied by Scanning Electron Microscope (SEM). MgO-FCN-NPs was investigated as a fiuoride sorbent by considering the combined effects of some significant parameters such as PH, adsorbent dose , contact time and F concentration by building a mathematical model that accurately describes the overall process. Fluoride removal by MgO-FCN-NPs were investigated using Box-Bhnken design in response surface methodology, that most common and efficient design. It has advantage such as reduction consumption, in the number of experiment and cost (25). Moreover, the experimental data were analyzed by Variance (ANOVA), R2 and lack of fit test to evaluate the significant of the model.

MATERIALS AND METHODS

Materials

Chemicals were used without further purification for this work. Sodium fluoride) NaF(, NaOH and H_2SO_4 (supplied by Sigma-Aldrich Co, Germany), $Mn(NO_3)_2.6H_2O$ (99%), $Co(NO_3)_2.6H_2O$ (99%), $Fe(NO_3)_3.6H_2O$ (99%) NaOH (98%), HCl (37%) were purchased from Merck.

Synthesis of MgO-FCN-NPs

MgO-FCN-NPs were produced using previously described method with little modification [26].

Characterization of MgO-FCN-NPs

SEM (Mira 3-XMU apparatus proficient of 700,000 x magnifications) was used to study morphology of nanoparticles

Batch study

A stock solution of fluoride (1000 mg/L) was prepared by dissolving sodium fluoride in distilled water, and certain concentrations of fluoride were obtained by further dilutions. The pH of each last solution was adjusted by adding 0.1N H_2SO_4 and 0.1N NaOH solution and the pH were measured using an MT65 pH meter. Following design of experiments, 100 ml of fluorine solution with different pHs, absorbent doses, contact times, and initial fluorine concentration was poured in 250-ml flasks, at room temperature, and mixing ratio of 120 rpm on a shaker. Fluorine concentrations with concentrations of interest were prepared through diluting the stock solution of fluorine. Once the contact time was finished, the samples were filtered using Whatman filter paper 0.45 μm, and the final absorption level of the solution was read at a maximum wavelength of 570 nm using spectrophotometer UV/Vis (Shimadzu Model: CE-1021-UK), and the removal efficiency (Y) was determined according to the following Equation (1).(27-29).

$$Y(\%) = \frac{C_0 - C_e}{C_0} * 100 \quad (1)$$

The amount of fluoride adsorbed per unit adsorbent (mg/g) was calculated according to a mass balance on the fluoride concentration using Equation (2):

$$Y(\%) = \frac{(C_0 - C_e)V}{m} \quad (2)$$

BOX-Behnken design method

Optimization of fluoride removal by the MgO-FCN-NPs was performed through surface response methodology via Box-Behnken model. The effect of four independent variables of pH, nanoparticle dose, contact time, and initial concentration was

Table 1. Coded and actual values of variable of the experimental design

Factor	Independent variables	Unit	Range and level of actual and coded values					
			Low Actual	High Actual	Low Coded	High Coded	Mean	Std. Dev.
A	Dose	g/L	0.02	0.1	-1	1	0.06	0.031
B	initial concentrations of fluoride	mg/L	10	50	-1	1	30	15.49
C	pH		3	11	-1	1	7	3
D	Contact time	min	30	180	-1	1	105	58.09

Table 2. CCD of two variables and their responses.

Run	Dose g/L	Concentration F	pH	Time	Flouride removal %
1	0.1	30	7	105	85.13
2	0.1	50	11	180	98.95
3	0.06	30	7	105	86.36
4	0.02	10	3	30	69.58
5	0.02	50	3	30	73.95
6	0.02	10	11	180	93.35
7	0.1	10	11	180	93.18
8	0.06	30	7	180	99.47
9	0.1	10	3	30	68.18
10	0.06	30	7	105	86.01
11	0.02	10	11	30	66.6
12	0.06	30	7	105	86.01
13	0.06	30	3	105	86.53
14	0.02	50	3	180	100
15	0.06	30	11	105	86.01
16	0.06	10	7	105	82.86
17	0.02	10	3	180	96.32
18	0.02	50	11	30	73.25
19	0.1	50	3	30	73.07
20	0.02	30	7	105	86.01
21	0.06	30	7	30	72.72
22	0.06	30	7	105	86.18
23	0.06	50	7	105	87.41
24	0.02	50	11	180	99.65
25	0.06	30	7	105	86.18
26	0.1	50	3	180	99.3
27	0.1	10	3	180	95.62
28	0.1	10	11	30	65.9
29	0.1	50	11	30	72.55
30	0.06	30	7	105	86.01

examined for defluorination, performed at five levels, according to Table 1.The percentage removal of fluoride as a response to each experiment and their predicted result is shown in Table 2.

By applying RSM method, the following equation which represents the experimental relationship between the tested variables and defluorination as coded was determined.

$$Y = b0 + b1A + b2B + b3C + b4D + b11A2 + b22B2 + b33C2 + b44D2 + b12AB + b13AC + b14AD + b23BC + b24BD + b34CD$$

Where, Y is the response variable of each of the levels of factors (removal percentage)

was therefore correlated to the set of regression coefficients (β):intercept (β0), linear (β1, β2, β3), quadratic coefficients (β11, β22, β33) and

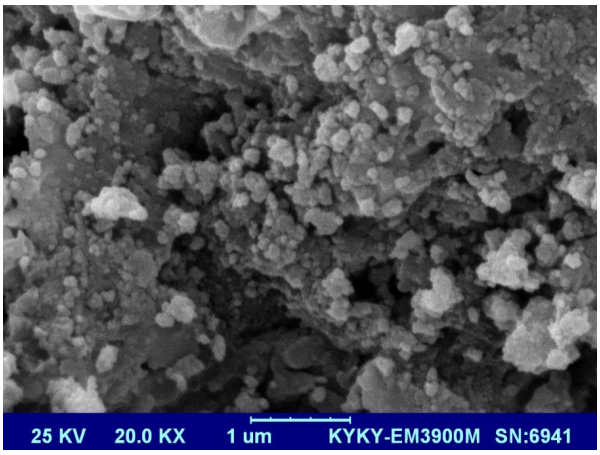

Fig.1. SEM image of nanoparticles

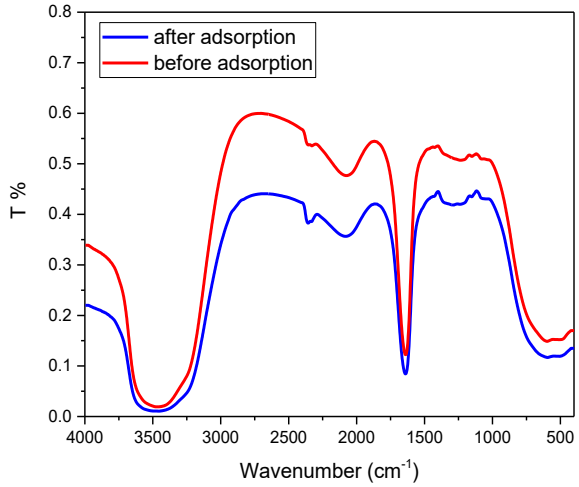

Fig. 2. FTIR spectra of fluoride and fluoride/nanoparticle

interaction(β12, β13, β23) .

The individual and interaction effects of the variables were designed using two- and three-dimensional plots(30,31).The quality of the polynomial equation fitting was evaluated using the coefficients obtained including R^2 and adjusted-R^2, in order to measure the most suitable model (32).

RESULTS AND DISCUSSIONS

Characterization of MgO-FCN-NPs

Morphology of MgO-FCN-NPs was characterized by SEM technique and SEM image of MgO-FCN-NPs is shown in Fig. 1.

The SEM image displays that the material consists of nearly spherical articles with changed sizes.

FTIR spectra of fluoride and fluoride/ nanoparticle is presented in Fig.2.

As seen in the Fig.2 related to fluoride/ nanoparticle, the absorption band at 657.73 cm^{-1} is related to M-O (M= Mn, Co, Fe) bond. The amine group (CH3-N-CH3) is dedicated to the absorption peak of 1640.6 cm^{-1}. Absorption band at 2068.65 cm-1 and broad band at 3459.14 cm-1 is related to the =C-H aromatic group and the – COOH group of Rhodamine B (The interaction of Rhodamine B with cluster structure) respectively. In Fig.2 related to before adsorption, the peak at 1548.34 cm-1 is assigned to the M-O bond, which was shifted to the right in the previous spectrum due to Rhodamine B of the electronegative electron groups, which was 657.73 cm-1. A absorption peak at 1662.95 cm^{-1} can be attributed to the structure of the – O-H is due to the M-OH bond and band at 3472.80 cm^{-1} was assigned to presence of H2O in the structure.

Table 3. ANOVA for Response Surface Quadratic Model

Source	Sum of Squares	df	Mean Square	F Value	p-value Prob > F	
Model	3377.00	14	241.21	2856.91	< 0.0001	significant
A-Dose	2.58	1	2.58	30.59	< 0.0001	
B-Concentration	120.14	1	120.14	1422.96	< 0.0001	
C-pH	9.55	1	9.55	113.12	< 0.0001	
D-Time	3200.93	1	3200.93	37911.43	< 0.0001	
AB	0.000	1	0.000	0.000	1.0000	
AC	0.12	1	0.12	1.45	0.2475	
AD	0.12	1	0.12	1.45	0.2475	
BC	4.78	1	4.78	56.56	< 0.0001	
BD	0.62	1	0.62	7.33	0.0162	
CD	7.641E-003	1	7.641E-003	0.090	0.7677	
A^2	1.78	1	1.78	21.12	0.0003	
B^2	4.16	1	4.16	49.24	< 0.0001	
C^2	0.044	1	0.044	0.52	0.4813	
D^2	0.24	1	0.24	2.86	0.1116	
Residual	1.27	15	0.084			
Lack of Fit	1.16	10	0.12	5.72	0.0341	significant
Pure Error	0.10	5	0.020			
Cor Total	3378.26	29				

Table 4. Model summary of the experimental design of fluoride adsorption from aqueous solution using MgO-FCN-NPs

Std. Dev.	0.29	R-Squared	0.9996
Mean	84.75	Adj R-Squared	0.9993
C.V. %	0.34	Pred R-Squared	0.9984
PRESS	5.48	Adeq Precision	165.732

DF: Degree of freedom, SS: Sum of Square, MS: Mean of Square.

RSM approach and statistical analysis

Statistical analysis of the results (RSM) lead to empirical relationship that mathematically express F removal percentage as function of interaction and individual contribution of variables.

The coefficients of Relation (12) were obtained using Minitab 16 software, whereby the following second order relation between the response variable and resulting independent variables after removal of parameters with minimal impact was obtained.

Final Equation in Terms of Coded Factors:

Fluoride removal =+123.36-0.58A+3.74B-1.08C+19.11D-0.047AB+0.17AC+0.078AD+0.73BC-0.23BD-0.016CD-1.17A^2-1.80B^2-0.17C^2-0.42D^2

The equation of fluoride removal indicates that the initial concentration of fluoride and contact time have had a positive effect and direct relationship on fluoride removal, and had a desirable effect on optimization. On the other hand, pH and absorbent dose have been negative, representing the inverse relationship between the parameter and response (33).To analyze the significance and the fitness of the obtained model, analysis of variance (ANOVA) is used. Table 3 presents the results of ANOVA (34).

R^2 shows that to what extent variability in the response variable can be explained by experimental factors and their interaction effects. R^2 predicted for fluoride was equivalent to (0. 0.9984), which had a logical proportion with R^2_{ADJ} (0.9993). Therefore, there was a good match between the values predicted by the model and the results obtained from the experiments. Furthermore, the obtained value (0.999) suggests that around 99.9% of the variability in the extent of removal has been justified by the independent variables. Comparison between the actual efficiency and predicted efficiency in the fluoride absorption process using MgO supported Fe-Co-Mn NPs has been presented in Table 4, revealing that there is a good and acceptable relationship between the obtained experimental values and the predicted values given the value of R^2.

Values of Prob>F at less than 0.05 showed the model terms are significant for F removal-value for the model is less than 0.05, confirming that the presented model can well predict experimental results.The results of second order regression

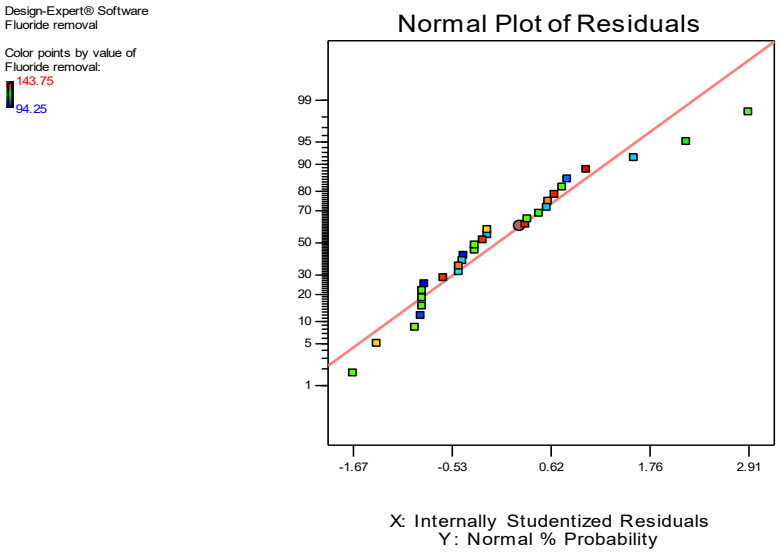

Fig. 3. The studentized residuals and normal % of probability residuals for defluoridation

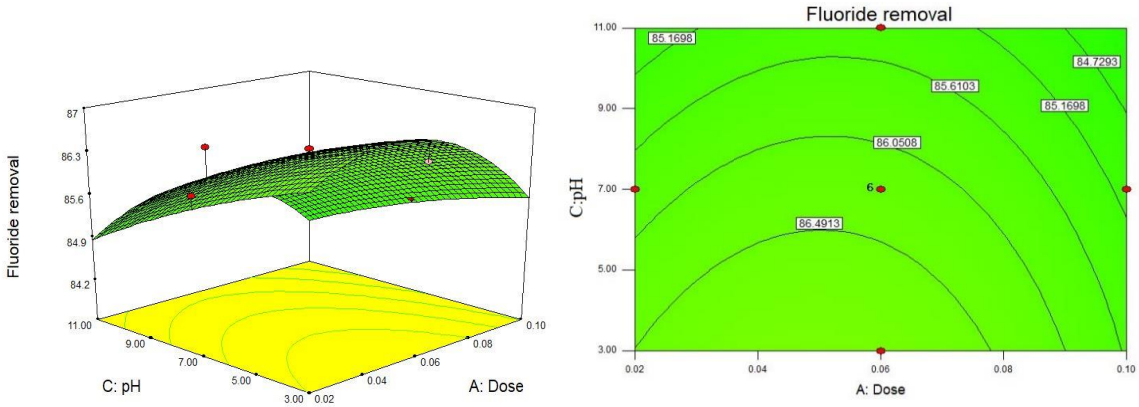

Fig. 4. 3D surface and 2D contour plot of the interactive effect of pH and dose on F removal efficiency by MgO-FCN-NPs at constant F concentration and time

model indicated that that second order model with Fmodel=2856.91 and prob>F<0.0001 was very significant (31).The lack-of-fit test compares the Pure error to residual error from replicated design points. The lack-of-fit F-value 0.0341 is significant as the p-value is < 0.05.

The coefficient of variations (CV) represents variability of the model results. A model is considered replicable if its CV is less than 10% (30). CV in this study has been 0.34, suggesting replication of the results obtained from the model (35). The difference between the response obtained from the experiment and response fitted by the model is called the residual. The points obtained from the experiment should lie on a straight line, whereby it can be concluded that the residual has a normal distribution (36). As can be observed in Fig.3, The residual has normal distribution.

Effect of interaction variales

The solution pH can affect dissociation of applied groups on the active sites of nanoparticles, structure of pollutants, and bonds of the nanoparticles surface (37).

Fig 4. Illustrates the two-dimensional and three-dimensional diagrams of the extent of removal as a function of nanoparticles dose and pH for performing the process with a solution at constant

concentration of fluoride 20 mg/L and contact time of 60 min, where the removal efficiency reached its maximum(99.9%) at pH=5 and nanoparticles dose of 0.05g/L

With an elevation of pH, fluoride removal efficiency from aqueous solutions decreases. Further, with the rise of the nanoparticles dose, Fluoride removal efficiency increased and reaches an optimal point. Thereafter, with elevation of the nanoparticles content, the removal efficiency will find a descending trend. The optimal value of the nanoparticles dose is obtained as 0.05g/L.

At acidic pHs, H^+ ions dominate the nanoparticles surface, whereby the nanoparticles surface finds a positive flux, the electrostatic attraction force between fluoride anions and nanoparticles surface grows, thereby enhancing the removal efficiency (27,38). At higher pHs and with accumulation of OH^+ ion on the nanoparticles surface, the repulsive force between the nanoparticles surface and fluoride ion increases, causing diminished efficiency (27,39). A similar result was reported by Vardhan and Srimurali(18).

Another influential parameter affecting the efficiency of contaminant removal processes is the absorbent dose. Fig.5, Fig.6 and Fig.7 demonstrate the effect of interactive parameter of MgO supported Fe-Co-Mn NPs dose and other variables. Here, the Defluoridation value first increased slightly with elevation of the nanoparticles dose from 0.02 to 0.05g/L (98.5-99.9%), After which with the rise of the MgO-FCN-NPs dose from 0.05 to 0.1g/L, the repulsive force between the nanoparticles results in inaccessibility of all active sites of the nanoparticles for the fluoride ion (27,40), where there removal efficiency reaches 94%.

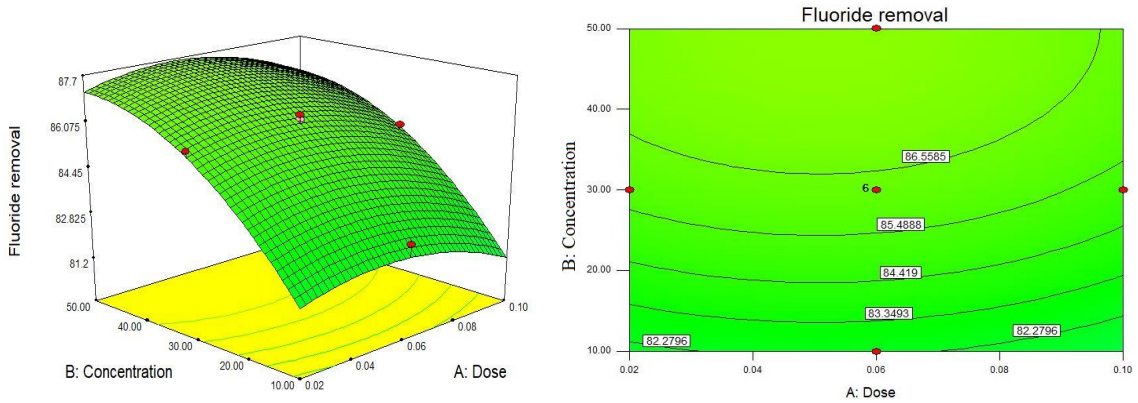

Fig. 5. 3D surface and 2D contour plot of the interactive effect of dose and F concentration on F removal efficiency by MgO-FCN-NPs at constant pH and time

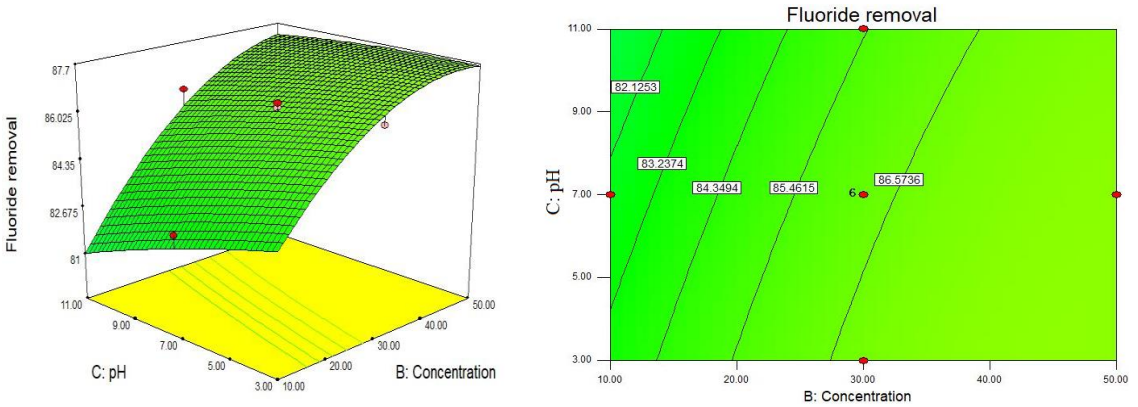

Fig. 6. 3D surface and 2D contour plot of the interactive effect of pH and F concentration on F removal efficiency by MgO-FCN-NPs at constant dose and time

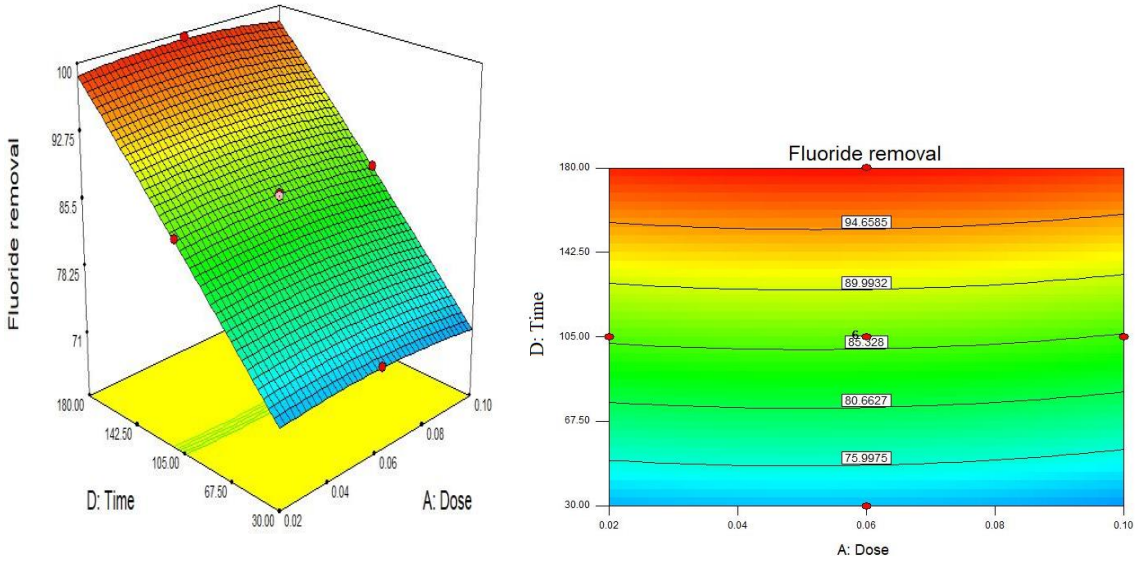

Fig. 7. 3D surface and 2D contour plot of the interactive effect of time and dose on F removal efficiency by MgO-FCN-NPs at constant F concentration and pH

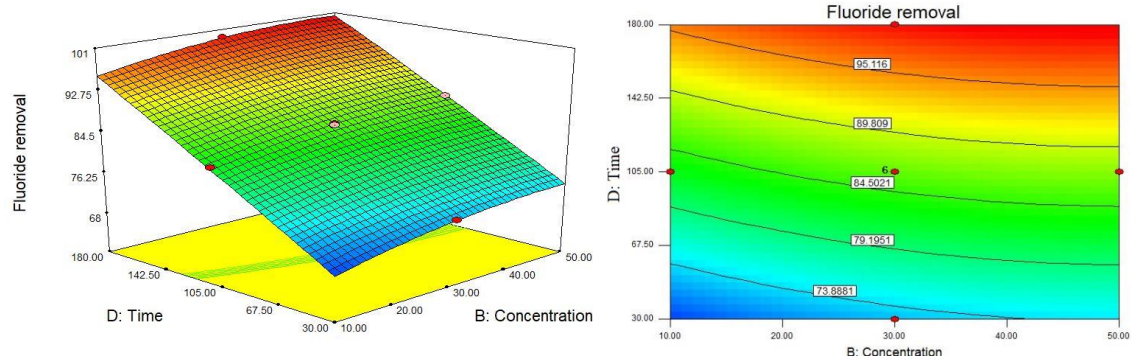

Fig. 8. 3D surface and 2D contour plot of the interactive effect of time and F concentration on F removal efficiency by MgO-FCN-NPs at constant dose and pH

Fluoride ion has been initially absorbed on the free sites of the nanoparticles at the beginning of the process 90 min(99%) at a high rate, and over time the removal efficiency did not have a considerable increase and remained almost constant.

At the beginning of the process, the entire surface of the absorbent has been active and fluoride solution concentration has been high. Therefore, they are rapidly absorbed by the active sites of the nanoparticles where a layer of fluoride ion has formed on the external surface of nanoparticles, which blocks the pores of the absorbent, and over time, absorption on the internal surface of nanoparticles becomes limited (41). With the rise in fluoride concentration, the removal efficiency grows due to the concentration of fluoride on the surface of nanoparticles and increase the probability of collisions between nanoparticles molecules and fluoride (42). Study conducted by Viswanathan and Menakshi, (2008) reported that fluoride removal was rapid in the first 40 minutes, followed by a constant amount, and also reported an increase in fluoride uptake by increasing fluoride concentration(43). Fig. 8 shows the simultaneous effect of time and initial fluoride concentration on the fluoride removal efficiency by MgO-FCN-NPs and also Fig. 9 shows the effect of time and pH on fluoride removal.

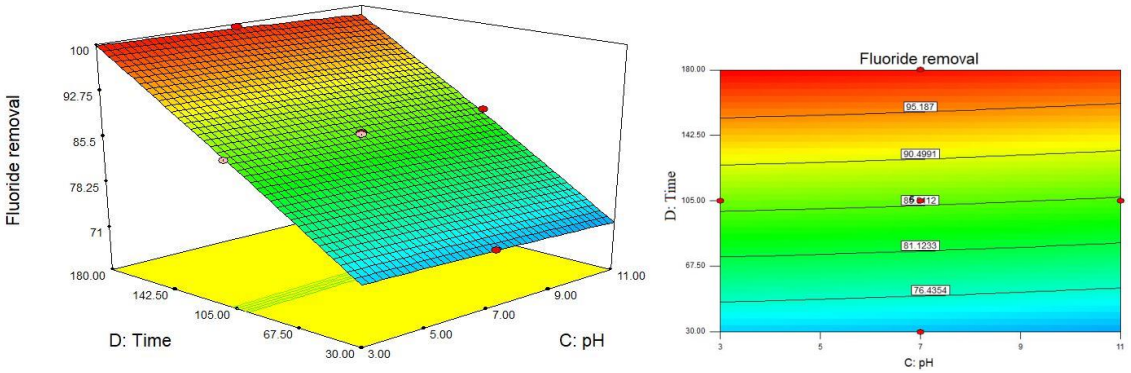

Fig. 9. 3D surface and 2D contour plot of the interactive effect of time and pH on F removal efficiency by MgO-FCN-NPs at constant F concentration and dose

Table 5. The Kinetic equationsed in the study (27,28,37)

Kinetic	Kinetic equations	plot	Parameters
pseudo-first-order	$log(q_e - q_t) = logq_e - \frac{k_1 t}{2.303}$	$log(q_e - q_t)\ vs\ t$	q_t (mg/g) is the amount of adsorbed fluoride on the adsorbed at time t k_1(1/min),is the rate constant of first-order adsorption, q_e(mg/g) the equilibrium sorption uptake
pseudo-second-order	$\frac{t}{q_t} = \frac{1}{k_2 q_e^2} + \frac{1}{q_e} t$	$\frac{t}{q_t}$ vs t	K_2(L/mg) is the rate constant of second-order model (mg/g min) q_e(mg/g) the equilibrium sorption uptake
intraparticle diffusion	$q_t = k_p t^{1/2} + C$	q_t vs $t^{0.5}$	k_p(mg/g $min^{0.5}$) is the intra-particle diffusion rate conatant and C (mg/g) q_t (mg/g) is the amount of adsorbed fluoride on the adsorbed at time t

Isotherm	**Isotherm equations**	**plot**	**Parameters**
Freundich	$Logq_e = \frac{1}{n}\log C_e + \log k_f$	Inq_evsInC_e	K_f(L/mg) for adsorption capacity n for adsorption intensity of fluoride on …nanoparticle, C_e(mg/L) is the equilibrium fluoride concentration in the solution q_e(mg/g) uptake at equilibrium
Langmuir	$\frac{1}{q_e} = \frac{1}{q_m} + (\frac{1}{q_m K_l})\frac{1}{C_e}$	$1/q_e$ vs $1/C_e$	q_e (mg/g) uptake at equilibrium, q_m(mg/g) maximum adsorption capacity C_e (mg/L) equilibrium concentration K_l(L/mg) is the adsorption equilibrium constant
Dubinin-Radushkevic	$\log q_e = \ln q_m - \beta\varepsilon^2$	Lnqe vs ε^2	q_e (mg/g) is the amount of fluoride adsorbed per unit of adsorbent, q_m(mg/g) is the theoretical adsorption capacity, β(mol^2/J^2) is the D-R constant and ε is the Polanyi potential
Temkin	$q_e = B \ln K_T + B \ln C_e$	q_e vs InC_e	K_T (L/mg)was the equilibrium binding constant related to the maximum binding energy, B(KJ/mol) was the activity coefficient related to the heat, C_e (mg/L) equilibrium concentration

Isotherm and kinetic modeling

Isotherm is a parameter representing the relationship between the concentration of the absorbate and the absorption capacity of the absorbent. In this study, Freundlich, Langmuir, and Temkin absorption isotherms have been used for mathematical modeling of the fluoride absorption process. After plotting different absorption diagrams, considering their correlation coefficients, it can be concluded which type of absorption

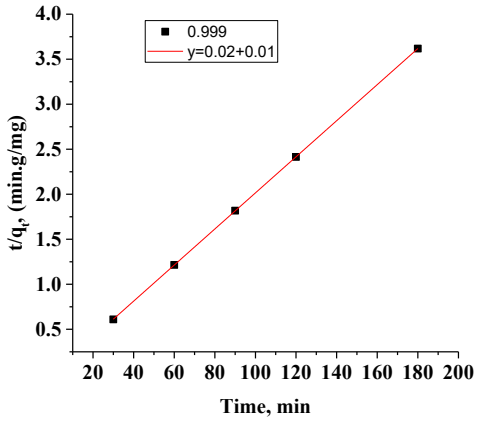

Fig. 10.

Table 6. Kinetic and Isotherm parameters for adsorption of F onto MgO-FCN-NPs for optimal condition

Isotherm model	Parameters		Kinetic model	Parameters	
Langmuir	(L/ mg) K_L	1.31	Pseudo- first order	K_f (1/min)	0.581277
	(mg/g) q_m	15.59		q_e (mg/g)	1.029201
	R^2	0.894		R^2	0.834
Freundlich	K_f(mg/g)	135.1	Pseudo-second order	K_2 (g/mg min)	0.036364
	n	0.47		q_e (mg/g)	50
	R^2	0.662		R^2	0.9999
Temkin	K_T	9.20196E-45	intra-particle diffusion	K (mg/g/min $^{1/2}$)	0.074
	B	0.01		C (mg/g)	48.81
	R^2	0.487		R^2	0.943
Dubinin-Radushkevich	β	5.181	Ritchie	K_r	2.5
	(mg/g) q_m	0.915		q_e (mg/g)	50
	R^2	0.691		R^2	0.871

curve has a great fit with experimental data of the absorption process.

Kinetic equations are used to describe the behavior of transfer of the molecules of the absorbate per unit of time on the surface of absorbent and investigating the variables affecting the reaction rate. In the present study, pseudo-first order and pseudo-second order plus interarticular effusion kinetic models have been used to investigate the factors affecting the reaction rate of fluoride absorption process on MgO-FCN-NPs.

The equations and parameters of isotherms and adsorption kinetics are presented in Table 5, and the values of isotherm parameters and fluoride absorption kinetics by the MgO-FCN-NPs have been calculated and presented in Table 6. The result reported that correlation coefficients (R^2) for Langmuir are more than another isotherm(0.894). So that indicated that the experimental data fitted well with the Langmuir model.

Optimization of the absorption process in removing fluoride by MgO-FCN-NPs

In order to obtain the optimal conditions for

Table 7. Optimal conditions for fluoride adsorption from aqueous solution using MgO-FCN-NPs.

Response	Name	Units	Obs	Analysis	Min	Max	Mean	Std. Dev.	Ratio
Y1	Fluoride removal	%	30	Polynomial	65.9	100	84.64	0.29	1.525

fluoride removal using the absorption process, the optimization process in a mixed search of level of variables at which the maximum fluoride removal occurs. Minitab software chooses the level of response during the best operational conditions within the range of operational variables of pH, nanoparticles dose, contact time, and initial concentration of input fluoride to the process and predicts them, as presented in Table 7.

To confirm the results obtained from the prediction of the model, an experiment was performed under optimal conditions. The results of the experiment had a good match with the extent of fluoride removal predicted by the model under optimal conditions.

CONCLUSIONS

The effect of parameters such as Ph, fluoride concentration, dose nanoparticle and time on adsorption fluoride by MgO-FCN-NPs can be well described by Quadratic model using response surface methodology based oneBox-Behnken design.The optimum values of the differences was determined in the adsorption process for fluoride the aqueous phase were 50 mg/L for initial F concentration, Ph 5for solution, and 0.05 g/L for dose MgO-FCN-NPs . The equilibrium data obtained for MgO-FCN-NPs

Is fitted to the Langmuir adsorption isotherms more than other model that indicated by higher correlation coefficient value of (). The values of the coefficient of determination, R^2 (0.9984) and the adjusted R^2 (0.9993) indicates that the process can be described by the RSM. The synthesized MgO-FCN-NPs have been applied successfully for the adsorptive removal of fluoride from its aqueous solution.

ACKNOWLEDGMENTS

The authors grateful to the Zabol University of Medical Sciences for the financial support of this study (Project No.IR.ZBMU.REC.1397.046).

CONFLICT OF INTEREST

The authors declare that there is no conflict of interests regarding the publication of this manuscript.

REFERENCES

1. Nigussie W, Zewge F, Chandravanshi BS. Removal of excess fluoride from water using waste residue from alum manufacturing process. Journal of Hazardous Materials. 2007;147(3):954-63.
2. Rafique A, Awan MA, Wasti A, Qazi IA, Arshad M. Removal of Fluoride from Drinking Water Using Modified Immobilized Activated Alumina. Journal of Chemistry. 2013;2013:1-7.
3. Mourabet M, El Rhilassi A, El Boujaady H, Bennani-Ziatni M, Taitai A. Use of response surface methodology for optimization of fluoride adsorption in an aqueous solution by Brushite. Arabian Journal of Chemistry. 2017;10:S3292-S302.
4. Suneetha M, Sundar BS, Ravindhranath K. Removal of fluoride from polluted waters using active carbon derived from barks of Vitex negundo plant. Journal of Analytical Science and Technology. 2015;6(1).
5. Erdal S, Buchanan SN. A Quantitative Look at Fluorosis, Fluoride Exposure, and Intake in Children Using a Health Risk Assessment Approach. Environmental Health Perspectives. 2005;113(1):111-7.
6. Bejaoui I, Mnif A, Hamrouni B. Performance of Reverse Osmosis and Nanofiltration in the Removal of Fluoride from Model Water and Metal Packaging Industrial Effluent. Separation Science and Technology. 2014;49(8):1135-45.
7. Hussain J, Sharma KC, Hussain I. Fluoride in drinking water and its ill affect on Human Health: A review. Journal of Tissue Research. 2004;4(2):263-73.
8. Rajkumar S, Murugesh S, Sivasankar V, Darchen A, Msagati TAM, Chaabane T. Low-cost fluoride adsorbents prepared from a renewable biowaste: Syntheses, characterization and modeling studies. Arabian Journal of Chemistry. 2019;12(8):3004-17.
9. Kofa GP, Gomdje VH, Telegang C, Koungou SN. Removal of Fluoride from Water by Adsorption onto Fired Clay Pots: Kinetics and Equilibrium Studies. Journal of Applied Chemistry. 2017;2017:1-7.
10. Tang Q-q, Du J, Ma H-h, Jiang S-j, Zhou X-j. Fluoride and Children's Intelligence: A Meta-analysis. Biological Trace Element Research. 2008;126(1-3):115-20.
11. Bhatnagar A, Kumar E, Sillanpää M. Fluoride removal from water by adsorption—A review. Chemical Engineering Journal. 2011;171(3):811-40.
12. Suneetha M, Sundar BS, Ravindhranath K. Removal of fluoride from polluted waters using active carbon derived from barks of Vitex negundo plant. Journal of Analytical Science and Technology. 2015;6(1).
13. Jorfi S, Rezaei Kalantary R, Mohseni Bandpi A, Jaafarzadeh Haghighifard N, Esrafili A, Alaei L. Fluoride removal from water by adsorption using bagasse, modified bagasse and chitosan. Iranian Journal of Health and Environment. 2011 May 15;4(1):35-48.
14. Razbe N, Kumar R, Kumar P, Kumar R. Removal of fluoride ion from aqueous solution. International Journal of

Computational Engineering Research. 2013 Apr;3(4):128-33.
15. Chakrabortty S, Roy M, Pal P. Removal of fluoride from contaminated groundwater by cross flow nanofiltration: Transport modeling and economic evaluation. Desalination. 2013;313:115-24.
16. Biswas G, Dutta M, Dutta S, Adhikari K. A comparative study of removal of fluoride from contaminated water using shale collected from different coal mines in India. Environmental Science and Pollution Research. 2015;23(10):9418-31.
17. Bejaoui I, Mnif A, Hamrouni B. Performance of Reverse Osmosis and Nanofiltration in the Removal of Fluoride from Model Water and Metal Packaging Industrial Effluent. Separation Science and Technology. 2014;49(8):1135-45.
18. Vivek Vardhan CM, Srimurali M. Removal of fluoride from water using a novel sorbent lanthanum-impregnated bauxite. SpringerPlus. 2016;5(1).
19. Maheshwari RC. Fluoride in drinking water and its removal. Journal of Hazardous materials. 2006 Sep 1;137(1):456-63.
20. Foo KY, Hameed BH. Insights into the modeling of adsorption isotherm systems. Chemical Engineering Journal. 2010;156(1):2-10.
21. Ali I, Gupta VK. Advances in water treatment by adsorption technology. Nature Protocols. 2006;1(6):2661-7.
22. Kumar E, Bhatnagar A, Ji M, Jung W, Lee S-H, Kim S-J, et al. Defluoridation from aqueous solutions by granular ferric hydroxide (GFH). Water Research. 2009;43(2):490-8.
23. Çengeloğlu Y, Kır E, Ersöz M. Removal of fluoride from aqueous solution by using red mud. Separation and purification Technology. 2002 Jul 1;28(1):81-6.
24. Jamode AV, Sapkal VS, Jamode VS, Deshmukh SK. Adsorption Kinetics of Defluoridation Using Low-Cost Adsorbents. Adsorption Science & Technology. 2004;22(1):65-73.
25. Ferreira SLC, Bruns RE, Ferreira HS, Matos GD, David JM, Brandão GC, et al. Box-Behnken design: An alternative for the optimization of analytical methods. Analytica Chimica Acta. 2007;597(2):179-86.
26. Davarpanah AM, Arsalanfar M. Study of different effects on magnetic properties of MgO-supported Fe–Co–Mn oxides. Applied Physics A. 2017;123(8).
27. Rahdar A, Ahmadi S, Fu J, Rahdar S. Iron oxide nanoparticle preparation and its use for the removal of fluoride from aqueous solution: application of isotherm, kinetic and thermodynamics. DESALINATION AND WATER TREATMENT. 2019;137:174-82.
28. Bazrafshan E, Kord Mostafapour F, Rahdar S, Mahvi AH. Equilibrium and thermodynamics studies for decolorization of Reactive Black 5 (RB5) by adsorption onto MWCNTs. Desalination and Water Treatment. 2014;54(8):2241-51.
29. Ahmadi S, Rahdar S, Igwegbe CA, Rahdar A, Shafighi N, Sadeghfar F. Data on the removal of fluoride from aqueous solutions using synthesized P/γ-Fe2O3 nanoparticles: A novel adsorbent. MethodsX. 2019;6:98-106.
30. Application of response surface methodology in the degradation of Reactive Blue 19 using H2O2/MgO nanoparticles advanced oxidation process
31. Parsa J, Abbasi M. Modeling and optimizing of sonochemical degradation of Basic Blue 41 via response surface methodology. Open Chemistry. 2010;8(5):1069-77.
32. Cevheroğlu Çıra S, Dağ A, Karakuş A. Application of Response Surface Methodology and Central Composite Inscribed Design for Modeling and Optimization of Marble Surface Quality. Advances in Materials Science and Engineering. 2016;2016:1-13.
33. Mourabet M, El Rhilassi A, El Boujaady H, Bennani-Ziatni M, Taitai A. Use of response surface methodology for optimization of fluoride adsorption in an aqueous solution by Brushite. Arabian Journal of Chemistry. 2017;10:S3292-S302.
34. Rahmani AR, Almasi H, Bajalan S, Rezaei Vahidian H, Zarei A, Shabanloo A. Optimization of Ciprofloxacin Antibiotic Sonochemical Degradation with Persulfate Activated by Nano Zero-Valent Iron by Central Composite Design Method. Journal of Health. 2017 Jul 15;8(3):231-45.
35. Ghafari S, Aziz HA, Isa MH, Zinatizadeh AA. Application of response surface methodology (RSM) to optimize coagulation–flocculation treatment of leachate using poly-aluminum chloride (PAC) and alum. Journal of Hazardous Materials. 2009;163(2-3):650-6.
36. Ghanim AN. Optimization of pollutants removal from textile wastewater by electrocoagulation through RSM. Journal of University of Babylon. 2014;22(2):375-87.
37. Bazrafshan E, Rahdar S, Balarak D, Mostafapour FK, Zazouli MA. Equilibrium and thermodynamics studies for decolorization of Reactive Black 5 by adsorption onto acid modified banana leaf ash. Iranian journal of health sciences. 2015 Aug 15;3(3):15-28.
38. Sujana MG, Mohanty S. Characterization and fluoride uptake studies of nano-scale iron oxide-hydroxide synthesized by microemulsion method. International Journal of Engineering, Science and Technology. 2011;2(8).
39. Mohammadnia M, Naghizadeh A. Surveying of kinetics, thermodynamic, and isotherm processes of fluoride removal from aqueous solutions using graphene oxide nano particles. Journal of Birjand University of Medical Sciences. 2016 Jan 1;23(1):29-43.
40. Ghorai S, Pant KK. Equilibrium, kinetics and breakthrough studies for adsorption of fluoride on activated alumina. Separation and Purification Technology. 2005;42(3):265-71.
41. Deshmukh WS, Attar SJ, Waghmare MD. Investigation on sorption of fluoride in water using rice husk as an adsorbent. Nature, Environment and Pollution Technology. 2009 Jun;8(2):217-23.
42. Muthu Prabhu S, Meenakshi S. Synthesis of metal ion loaded silica gel/chitosan biocomposite and its fluoride uptake studies from water. Journal of Water Process Engineering. 2014;3:144-50.
43. Sairam Sundaram C, Viswanathan N, Meenakshi S. Uptake of fluoride by nano-hydroxyapatite/chitosan, a bioinorganic composite. Bioresource Technology. 2008;99(17):8226-30.